Multiple effects of the cellular prion protein on tooth development

YAN ZHANG[1,#], SEONG-OH KIM[1,2,#], SIBYLLE OPSAHL-VITAL[1,3,] SUNITA P. HO[4],
JEAN-BAPTISTE SOURON[3], CHARLES KIM[1], KURT GILES[5,6] and PAMELA K. DEN BESTEN*[,1]

[1]Department of Orofacial Sciences, University of California San Francisco, USA, [2]Department of Pediatric Dentistry,
Oral Science Research Center, College of Dentistry, Yonsei University, Seoul, Korea, [3]University Paris Descartes,
EA2496, AP-HP, France, [4]Division of Biomaterials and Bioengineering, Department of Preventive and Restorative
Dental Sciences, [5]Institute for Neurodegenerative Diseases and [6]Department of Neurology,
University of California San Francisco, USA.

ABSTRACT The role of the prion protein (PrP) in transmissible spongiform encephalopathies has been the focus of intense investigation. However, less is known about the physiological function of normal cellular PrP (PrP^C). In adult human teeth, PrP^C has been identified in odontoblasts, cementoblasts and epithelial remnants of Malassez. In this study, we have localized PrP^C in developing human and mouse teeth, and investigated the function of PrP using a PrP-knockout (*Prnp*$^{0/0}$) mouse model. PrP^C was detected in developing human and mouse ameloblasts and odontoblasts. *In vitro,* undifferentiated dental mesenchymal cells from embryonic day 18 (E18) *Prnp*$^{0/0}$ mouse molars proliferated much more rapidly compared to age-matched, wild-type (wt) mouse molar dental mesenchymal cells. Histochemistry and immunohistochemical analyses showed a subtle but measurable phenotype, with the absence of PrP resulting in earlier initiation of both dentin and enamel formation. Consistent with this finding, laser microdissected odontoblasts from newborn *Prnp*$^{0/0}$ mouse incisors had a reduced proliferation rate, as measured by the expression of proliferating cell nuclear antigen (PCNA), and increased type 1 collagen mRNA expression. Dentin microhardness of the fully erupted molars was reduced and incisal enamel mineralization was delayed in *Prnp*$^{0/0}$ compared to age-matched *wt* mouse teeth. Taken together, these results suggest that PrP^C affects multiple processes involved in tooth formation, through regulating the differentiation of ameloblasts and odontoblasts.

KEY WORDS: *tooth development, prion protein, ameloblast, odontoblast*

Introduction

The prion protein (PrP) is a glycophosphatidylinositol-anchored glycoprotein. It is highly conserved among mammals and is also present in birds, reptiles and amphibians (Premzl and Gamulin 2007), suggesting an important functional role. Normal cellular PrP, termed PrP^C, is widely expressed in adult tissues, predominantly in neuronal cells, and its expression is regulated both embryonically (Manson *et al.,* 1992, Tremblay *et al.,* 2007) and postnatally (Lazarini *et al.,* 1991, McKinley *et al.,* 1987). However, mice in which PrP expression has been genetically abrogated are not only viable, but appear to have only subtle phenotypes (Bueler *et al.,* 1992, Manson *et al.,* 1994a).

Expression of PrP^C was detected in inner and outer epithelial layers of the E16.5 mouse tooth primordium by *in situ* hybridization (Manson *et al.,* 1992), and in the dental papilla and ameloblasts of E18.5 mice by immunohistochemistry (Khan *et al.,* 2010). PrP^C was also detected in odontoblasts, cementoblasts and epithelial remnants of Malassez in adult human dental tissues by immunohistochemistry (Schneider *et al.,* 2007). These cells are all involved in the formation of mineralization tissues. In mice infected with the Me7 prion strain, the pathological isoform of the prion protein, PrP^{Sc}, was observed in the rests of Malassez lining the tooth surface (Okada *et al.,* 2010).

Teeth form through sequential reciprocal signaling interactions between ectodermal-derived dental epithelial cells and cranial neurocrest differentiated mesenchymal cells (Sharpe 2001, Thesleff

---

---

*Address correspondence to: Pamela DenBesten. 513 Parnassus Ave, San Francisco, CA 94143-0422, USA. Tel: +1-415-502-6383. Fax: +1-415-476-4204.
e-mail: pamela.denbesten@ucsf.edu # Note These authors contributed equally to this work.
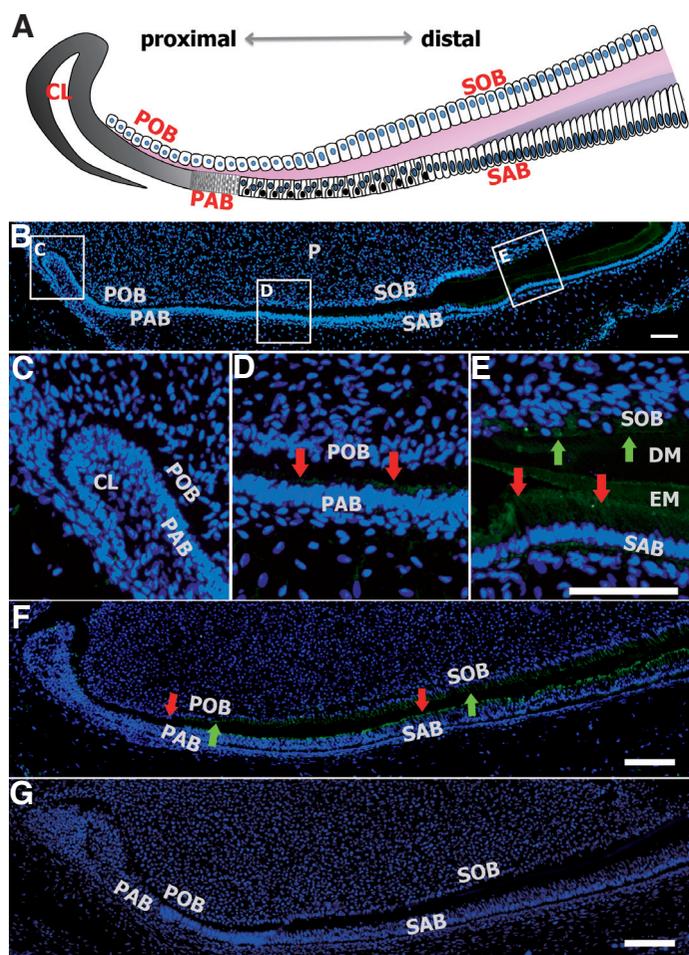
Fig. 1. Immunohistochemical staining of PrP in human fetal (B-E) and mouse (F,G) tooth organs. (A) *The diagram illustrates the dynamic development of dental mesenchymal cells and dental epithelial cells during incisor morphogenesis. The dental mesenchymal cells adjacent to epithelial cells develop into polarized pre-odontoblasts (POBs) first, then continuously develop into secretory odontoblasts (SOBs), which secret dentin matrix and are responsible for the dentin formation. The dental epithelial precursor cells located in the cervical loop (CL) migrate to the basal layer around the outside of the loop. The basal epithelial cells polarize and elongate to become pre-ameloblasts (PABs), then differentiate into secretory ameloblasts (SABs), which secrete enamel matrix proteins and attract minerals to initiate enamel biomineralization.* **(B)** *Staining of human developing incisor tooth organ showed significant upregulation of PrP (green staining) as the cells entered the secretory stage.* **(C)** *Higher magnification of the cervical loop (CL) area showed no PrP signal was detected.* **(D)** *Gradually increased PrP staining was detected first in pre-ameloblasts (PAB; red arrows).* **(E)** *PrP signal was observed in the fully differentiated secretory ameloblasts (SAB; red arrows), and secretory odontoblasts (SOB; green arrows).* **(F)** *In the mouse incisor, immunopositive PrP signal first appeared in pre-odontoblasts (POB; green arrows). The signals became more intense as the cells differentiated into SOB (green arrows) and SAB (red arrows).* **(G)** Prnp$^{0/0}$ *mouse incisors were immunonegative for PrP. All the blue stain is the counterstaining of nuclei with Hoechst 33324. Bars = 100 μm, bar in E applies to C and D. Pre-odontoblasts (POB), pre-ameloblasts (PAB), secretory odontoblasts (SOB), secretory ameloblasts (SAB), dental pulp (P), cervical loop (CL), dentin matrix (DM), enamel matrix (EM).*

and Nieminen 1996). Tooth formation initiates as the oral epithelial cells, lining upper and lower jaws in the first arch at the presumptive tooth sites, proliferate and thicken to form primary epithelial bands (also named dental placode). Proliferating epithelial cells invaginate into the underlying dental mesenchyme. In response to signals from the dental epithelium, the dental mesenchyme condenses and forms a bud structure (Bei and Maas 1998, Mandler and Neubuser 2001, Neubuser *et al.,* 1997). The epithelium then forms a cap-like structure overlying the dental mesenchyme.

Individual tissues in the tooth continue to differentiate during the subsequent bell stage (mouse E16 to postnatal days). As cusp morphogenesis continues, cytodifferentiation begins and mesenchymal cells lining the dental papilla differentiate into

columnar odontoblasts. As long as the odontoblasts begin to secrete dentin matrix, the adjacent pre-ameloblasts differentiate into ameloblasts (Harada *et al.,* 1999). Enamel mineralization begins as soon as secretory ameloblasts secrete amelogenins and other non-amelogenin proteins, all of which self-assemble to form a mineralizing enamel matrix on the dentin surface. At the transition between secretion and maturation stages, matrix proteins are rapidly removed by matrix proteinases leaving a porous enamel matrix. This matrix is subsequently completely mineralized as maturation stage ameloblasts modulate between smooth and ruffle bordered cells. At the end of enamel maturation, ameloblasts undergo apoptosis and finally disappear as the tooth erupts (Vaahtokari *et al.,* 1996).

In this study, we first localized PrP^C in human developing incisors and mouse teeth at various developmental stages, then further investigated the role of PrP^C on tooth development by using mouse tooth models. Mouse molars are rooted teeth similar to human teeth, while mouse incisors are continuously growing, allowing studies of all stages of tooth formation in a single tooth. PrP-knockout (*ko*; *Prnp$^{0/0}$*) mice and wild-type (*wt*) mice were used to investigate the physiological function of PrP in tooth development. Cell proliferation and differentiation was
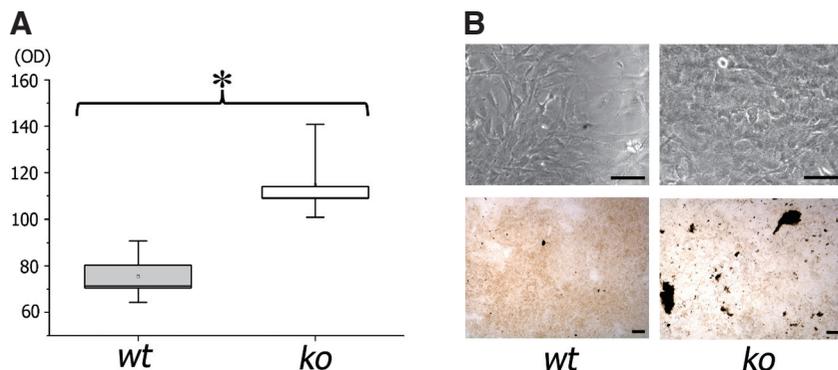

Fig. 2. The effect of PrP on undifferentiated dental mesenchymal cells (DMCs) isolated from E18 mouse molars. (A) *DMCs from* Prnp$^{0/0}$ *(ko) mice proliferated faster, as indicated by the significantly increased optical density (OD) compared to cells isolated from* wt *mice (*p<0.05, n=4; Student's t-test) based on the BrdU cell proliferation assay.* **(B)** *The top panels showed that DMCs from* Prnp$^{0/0}$ *mice plated at the same density as* wt *cells, were more confluent after 5 days in culture (Bars = 10 μm). The lower panels showed von Kossa staining of DMCs grown for 2 wks in mineralizing media, and demonstrated the increased mineralization of DMCs isolated from* Prnp$^{0/0}$ *compared to* wt *mice (Bars = 100 μm). Representative results from three independent experiments.*

compared in developing dental mesenchymal cells isolated from E18 *wt* and *ko* mice, as well as in differentiated pre-odontoblasts and secretory odontoblasts microdissected from newborn *wt* and *ko* mice. The progressive formation of dentin and enamel were investigated in newborn mouse incisors, and microhardness was measured in fully formed first mouse molars.

The results of this study showed that PrP^C had the specific effects on different stages of tooth cell differentiation and matrix mineralization. The primary phenotypes in *Prnp*$^{0/0}$ mice included enhanced pulp mesenchymal cell proliferation and mature dentin with a reduced hardness. Enamel mineralization was initiated

earlier, followed by a subsequent delay in final mineralization. These effects suggest that PrP^C may be involved in mediating differentiation of the cells responsible for tooth hard tissue formation.

Results

Prion protein (PrP) was localized in both odontoblasts and ameloblasts of developing teeth

In developing human teeth, immunohistochemical analysis showed PrP^C localized at the apical border of pre-ameloblasts and secretory ameloblasts, but not apparent in the developing dental mesenchyme until the secretory stage of dentin formation (Fig. 1 B-E). In the continuously growing mouse incisor, positive PrP^C immunostaining was first detected in pre-odontoblasts, and became more intense as the cells differentiated to secretory stage (Fig. 1F). The positive immunostaining signal was also detected
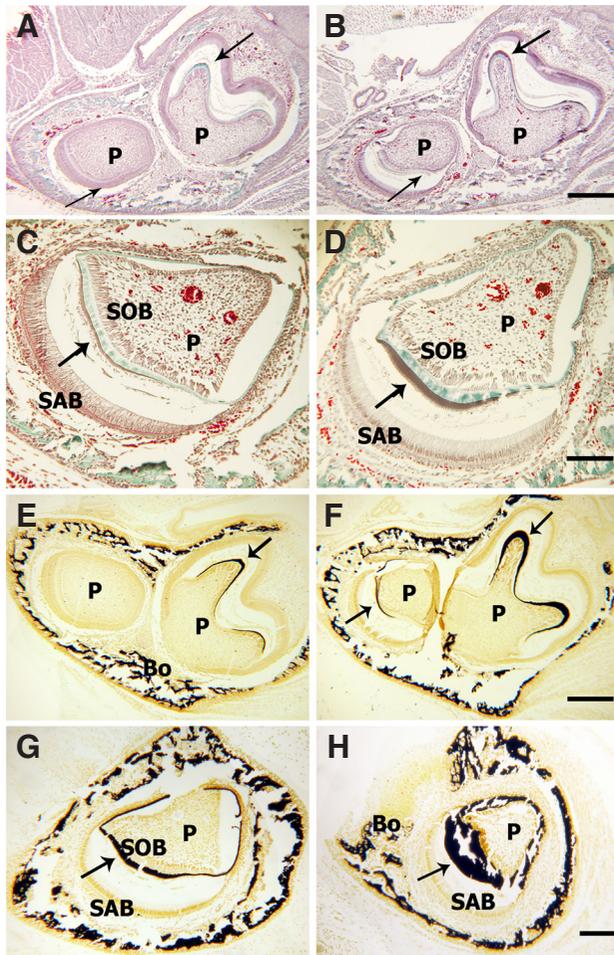

Fig. 3 (Left). Histological comparisons of newborn *wt* (A,C,E,G) and *Prnp*$^{0/0}$ (B,D,F,H) mouse mandibles. *Newborn mouse mandibles were collected, fixed, embedded, and cut into 7μm -thick transversal sections. Sections at the same distance from the incisal tip were examined and compared. H&E staining of the* wt *mouse mandibles* **(A)** *showed dentin (green; indicated by arrow) but no enamel matrix formation was visible in molar, and no dentin or enamel formation was detected on the underlying cross section of the incisor (indicated by arrow). However, in the* Prnp$^{0/0}$ *mouse* **(B)** *enamel matrix had begun to form on the molar (red) and dentin matrix (green) had begun to form on the underlying incisor (indicated by arrows). Trichrome staining* **(C,D)** *showed a greater width of enamel (brown) and dentin (green) (indicated by arrows) in the* Prnp$^{0/0}$ *mice* **(D)** *as compared to* wt *mice* **(C)**. *Correlated to this increase in the matrix secretion, von Kossa staining showed increased mineralization in the enamel and dentin matrices (indicated by arrows) of* Prnp$^{0/0}$ **(F,H)** *compared to* wt *mice* **(E,G)**. *Bars: B = 500μm, D = 100μm, F = 500μm, H= 200μm, and apply to panels A, C, E and G respectively. Secretory ameloblast (SAB), secretory odontoblast (SOB), bone (Bo) and dental pulp (P).*
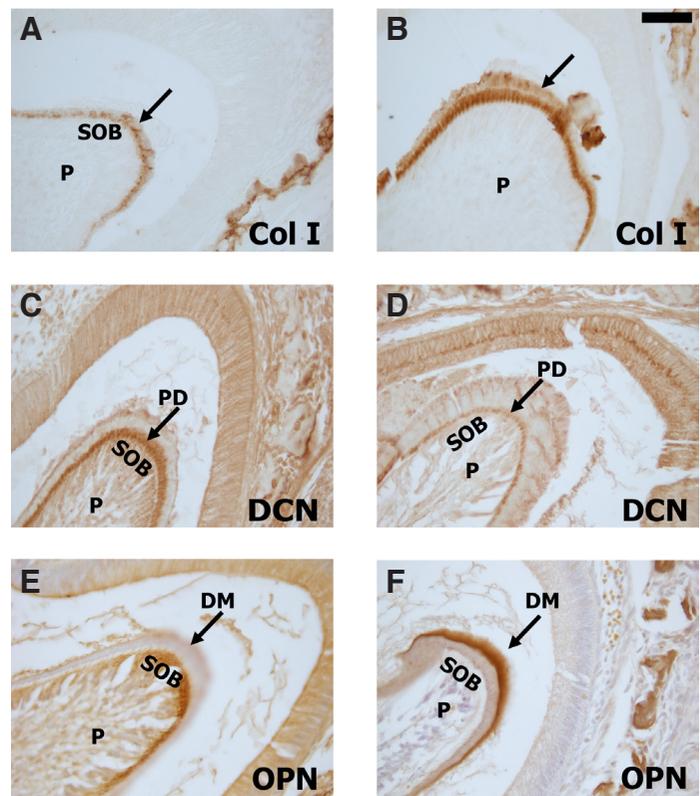
Fig. 4 (Right). Immunohistochemical staining of type I collagen (Col I), decorin (DCN) and osteopontin (OPN) in newborn *wt* (A,C,E) and *Prnp*$^{0/0}$ (B,D,F) molars. *Staining of* Prnp$^{0/0}$ *mouse molars showed increased type I collagen immunolabeling in odontoblasts and dentin matrix* **(B)** *(indicated by arrows) compared to* wt *molars* **(A)**. *The predentin (PD) stained positive for decorin* **(C,D)** *(indicated by arrows), with decreased immunostaining in the* Prnp$^{0/0}$ *mouse molars* **(D)**. *Anti-osteopontin antibody was localized in the dentin matrix (indicated by arrows), and was increased in the* Prnp$^{0/0}$ *mouse molar* **(E)** *compared to* wt *molar* **(F)**. *Bar in B=100μm and applies to all panels. Secretory odontoblast (SOB), dental pulp (P), predentin (PD) and dentin matrix (DM).*
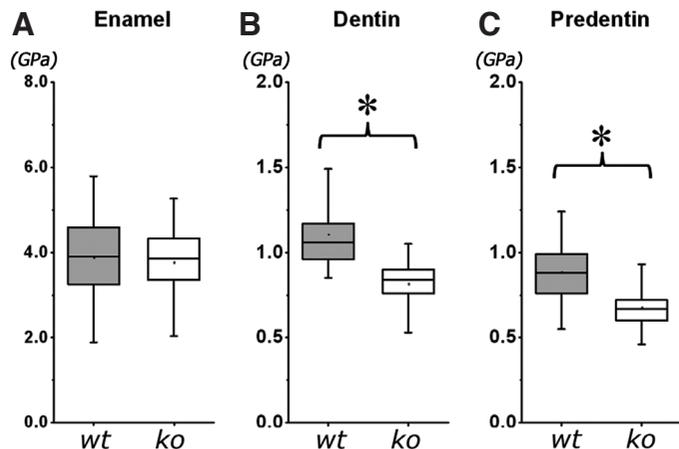
Fig. 5. Microhardness of enamel, dentin and predentin in adult mouse molars, determined by microindentation. *Although there was no significant difference in enamel hardness* **(A)**, *the dentin* **(B)** *and predentin* **(C)** *of* Prnp⁰ᐟ⁰ *(ko) mice had a significantly decreased hardness compared to* wt *mice (*p<0.05, n=6; Student's t-test).*

in the secretory ameloblasts. There was no signal for PrP^C in the *Prnp^{0/0}* mouse (Fig. 1G).

Dental mesenchymal cells isolated from E18 Prnp^{0/0} mouse molars had increased proliferation rate, leading to more rapid mineral formation in vitro

Analysis by BrdU immunoassay showed that embryonic dental mesenchymal cells derived from E18 *Prnp^{0/0}* mouse molars had enhanced proliferative activity compared to age-matched *wt* control cells (p<0.05, n=4) (Fig. 2A). When the cells were grown

in mineralization media for 2 wks, the more rapidly proliferating cells isolated from *Prnp^{0/0}* mice, differentiated sooner and formed more mineralizing nodules as indicated by increased von Kossa staining (Fig. 2B).

Early initiation of odontoblast and ameloblast cell differentiation and matrix apposition were detected in newborn Prnp^{0/0} mouse teeth

Cross-sections of mouse mandibles, taken at the same distance from the incisal tips, showed earlier initiation of dentin and enamel formation in *Prnp^{0/0}* mice compared to the *wt* mice (Fig. 3 A,B). Sections slightly more incisally located, at a later stage of matrix secretion, showed that the *Prnp^{0/0}* mice had a relatively thicker enamel matrix (Fig. 3 C,D), and a more mineralized dentin matrix compared to *wt* mice (Fig. 3 E-H). These results were confirmed on three independent samples of *Prnp^{0/0}* and *wt* mice.

Type I collagen immunostaining signal was increased in the *Prnp^{0/0}* newborn mouse odontoblasts and dentin matrix (Fig. 4 A,B). Immunostaining signals for decorin in predentin were reduced in the *Prnp^{0/0}* mouse teeth compared to *wt* (Fig. 4 C,D), whereas osteopontin was increased in the *Prnp^{0/0}* mouse dentin matrix (Fig. 4 E,F). These results were confirmed in three sets of independent samples. qPCR analysis on laser microdissected pre-odontoblasts and secretory odontoblasts also showed enhanced differentiation of *Prnp^{0/0}* odontoblasts with a 27 fold reduction in PCNA, a 1.4 fold increase in type I collage expression, and a 2.1 fold increase in DSPP as compared to *wt* secretory odontoblasts (Table 1).

Dentin of adult Prnp^{0/0} mouse molars had reduced hardness

Microhardness of enamel from sagittally sections of adult mouse molars was not significantly different between *Prnp^{0/0}* and *wt* mice (n=6) (Fig. 5A). However, the microhardness of both dentin and predentin was significantly lower in *Prnp^{0/0}* mouse molars compared to *wt* mouse molars (p<0.05, n=6) (Fig. 5B,C).

Enamel mineralization in Prnp^{0/0} mouse incisors was delayed

A stereoscopic analysis of ground sagittal sections showed a significantly increased length of the more porous zone in the continuously erupting *Prnp^{0/0}* mouse incisors (p<0.05, n=6) (Fig. 6E). This zone represents the partially mineralized matrix at the transition stage between the protein-rich secretory stage of enamel and the mineralized maturation stage of enamel. A microCT analysis also showed a significant increase in the length
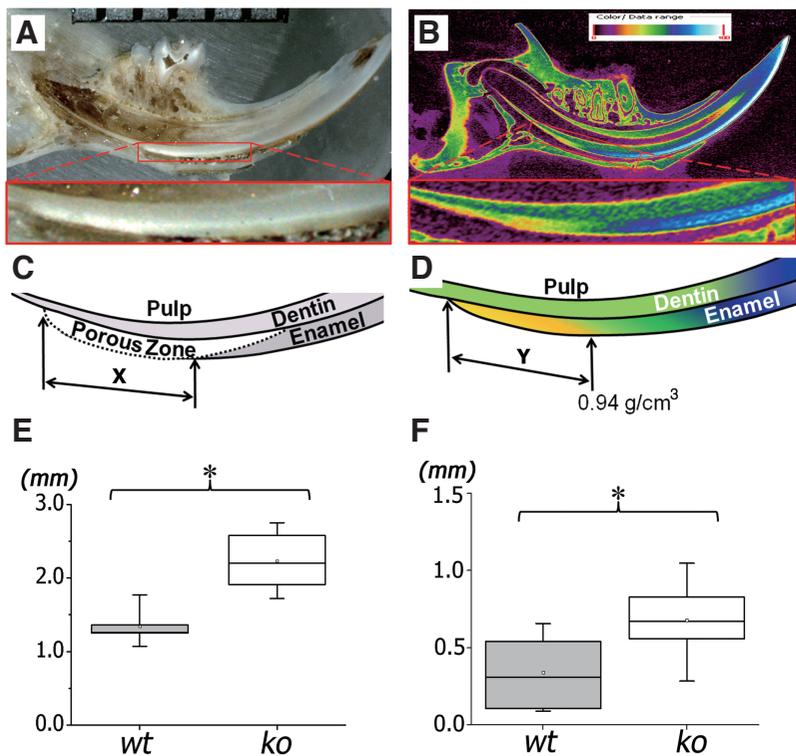

Fig. 6. Sagittal sections of mandibular incisors showed an increased length of early mineralizing zones in enamel of Prnp^{0/0} (ko) mice by both stereomicrospcopy (A,C,E), and microCT (B,D,F). (A) *Representative stereomicroscopic image showed the white opaque zone, which occurs when the secretory matrix proteins are removed, leaving an increased porosity zone prior to final mineralization.* **(B)** *A representative microCT image taken at the center of a sagittal view of a hemimandible. Length of the porous zone "X", shown schematically in* **(C)** *was significantly increased in the* ko *incisors as compared to* wt *incisors* **(E)**. *Similarly, length of the zone "Y" from the first detectable mineralizing matrix to the point with a relative density 0.94 g/cm³ of a developing incisor* **(D)** *was significantly increased in the* ko *incisors compared to* wt *mice* **(F)** *(* p<0.05, n=6; Student t-test).*

TABLE 1

**FOLD DIFFERENCE OF mRNA EXPRESSION
IN PRE-ODONTOBLASTS (POB) AND SECRETORY
ODONTOBLASTS (SOB) MICRODISSECTED
FROM *Prnp$^{0/0}$ (ko)* AND *wt* NEWBORN MOUSE INCISORS**

Fold Difference	PCNA	Type I collagen	DSPP
POB (*ko/wt*)	0.88 ± 0.07	1.85 ± 0.02	4.17 ± 0.02
SOB (*ko/wt*)	0.037 ± 0.17	1.41 ± 0.03	2.13 ± 0.02

Data are the averages of two independent samples, each measured in triplicate. The standard deviation (indicated by ±) for all 6 measurements is included as an indication of reproducibility.

of the early mineralizing (secretory stage) enamel in the *Prnp$^{0/0}$* mouse incisor compared to the *wt* controls (p<0.05, n=6) (Fig. 6F). This analysis was further confirmed by a cross-sectional imaging analysis of the forming mouse incisor enamel (data not shown).

Discussion

PrP is primarily expressed in the CNS, though modest expression can also be detected in the peripheral nervous system and non-neuronal tissues (Caughey *et al.,* 1988, Li *et al.,* 2001, Manson *et al.,* 1992). Although much is known about the pathologic isoform of PrP, termed PrP^{Sc}, the physiological role of normal cellular PrP^{C} remains poorly defined (Aguzzi *et al.,* 2008, Chiesa and Harris 2009). The generation of mouse lines devoid of PrP (*Prnp$^{0/0}$*) demonstrated that PrP is essential for prion propagation (Bueler *et al.,* 1993, Manson *et al.,* 1994b, Prusiner *et al.,* 1993). There were no gross abnormalities initially observed in *Prnp$^{0/0}$* mice, however subsequently, subtle and in some cases disputed phenotypic deficits were reported (Collinge *et al.,* 1994, Lledo *et al.,* 1996). Recent suggestions for PrP^{C} function include roles in olfaction (Le Pichon *et al.,* 2009), membrane transport (Fuhrmann *et al.,* 2006), maintenance of peripheral myelin (Bremer *et al.*), and regulating self-renewal and differentiation status of stem cells (Lee and Baskakov 2010).

Our observations reported in this study are consistent with the previous findings that PrP^{C} is localized in human and mouse odontoblasts (Manson *et al.,* 1992, Schneider *et al.,* 2007), as well as secretory ameloblasts in the developing tooth organ (Khan *et al.,* 2010). However, our immunolocalization analysis showed PrP^{C} highly localized in the apical border as well as lateral cell membranes, particularly in secretory odontoblasts and ameloblasts. This location may suggest a potential role of PrP related to cross-membrane transport or signaling transmission.

The tooth organ is a unique system containing neural crest derived mesenchyme and ectoderm derived epithelia that differentiate through reciprocal signaling interactions to form the mineralized dentin and enamel tissues. Dentin, formed by the mesenchymally derived odontoblasts is a collagenous mineralized tissue with many of the similar characteristics as bone. Enamel is the only mineralized epithelial-derived tissue in the human body, and is initially formed as a protein matrix. Enamel matrix proteins immediately attract minerals to initiate mineralization. Enamel proteins are then removed through the actions of proteinases and the overlying ameloblasts, which commit apoptosis as teeth erupt. A hard acellular mineral enamel structure is formed to protect dentin and pulp complex. As described in this study, we used the tooth organ to identify the effects of PrP^{C} on epithelially and mesenchymally

derived mineralized tissues throughout their differentiation and mineralization.

We used both molars and incisors to investigate the roles of PrP^{C} on the different tissues at various stages of tooth formation. Embryonic stage dental mesenchymal cells were compared *in vitro* for proliferation and differentiation. Dentin formation and mineralization was examined in the unerupted newborn mouse molar, and the fully formed dentin was characterized in erupted mouse molars. Enamel formation was characterized using the continuously erupting incisor where all stages of enamel formation can be identified within a single tooth.

We found stage-specific effects of PrP^{C} on tooth organ development. In the dental mesenchyme, when the undifferentiated dental mesenchymal cells lacking PrP were grown *in vitro,* the cells were highly proliferative compared to the age-matched *wt* mouse dental mesenchymal cells. When these cells were cultured in a mineralizing media, they formed more mineralizing nodules. This increased nodule formation by *Prnp$^{0/0}$* embryonic dental mesenchymal cells is likely to be related to their increased proliferation rate, leading to earlier confluence and cell differentiation *in vitro*.

This observation that rapid dividing dental mesenchymal cells leading to earlier cell differentiation also was evidenced by our observation from the effects of PrP^{C} on early dentin, as well as enamel differentiation and matrix maturation in animal model. In newborn mouse molars and incisors lacking of PrP resulted in earlier dentin and enamel matrix formation. This earlier formation of the dentin matrix was also evidenced by increased immunostaining for type 1 collagen and osteopontin, both of which are related to dentin matrix formation and mineralization. Similarly a reduction of decorin in the predentin layer is correlated with dentin maturation (Waddington *et al.,* 2003). qPCR analysis of mRNA isolated from odontoblasts (terminal differentiated dental mesenchymal cells) microdissected by LCM from cryosectioned newborn mouse incisors, showed increased expression of collagen type I, DSPP and reduced PCNA, also consistent with enhanced odontoblast differentiation. Final dentin formation in the *Prnp$^{0/0}$* mice had a reduced microhardness as compared to *wt* mice, even though dentin mineralization was initiated earlier in tooth formation.

Although there was also earlier mineralization of secretory stage enamel in *Prnp$^{0/0}$* mice, the length of the secretory and transition stages of the *Prnp$^{0/0}$* mouse enamel formation was longer, with the end result being no difference in final enamel density. This finding that there was no effect of PrP on final enamel mineralization was confirmed by the lack of any change in microhardness of molar enamel.

The varying effects of PrP at different stages of mineralizing tooth tissue formation, point to a common mechanism, potentially related to the altered intracellular calcium regulation. In bone marrow stromal cells, PCNA expression declines when the intracellular calcium concentration is increased (Ichikawa and Gemba 2009). The similarities between bone marrow stromal cells and dental mesenchymal cells in gene regulation and fate determination (Menicanin *et al.*), suggest that the increased proliferation rate of undifferentiated *Prnp$^{0/0}$* dental mesenchymal cells may also relate to PrP modulation of intracellular calcium (Beraldo *et al.,* Kagenishi *et al.,* 2009).

Although the role of calcium in the initiation of tooth tissue cell differentiation is not well defined, the location of PrP at the apical border of both secretory ameloblasts and odontoblasts is consis-

tent with the hypothesis that this protein is related to Ca^{2+} transport (Fuhrmann *et al.,* 2006), or regulating Ca^{2+} homeostasis (Powell *et al.,* 2008).

An interesting application of these studies is the potential to manipulate PrP expression in dental mesenchymal cells, to enhance proliferation in sites of injury. In pulp injury secondary to dental caries or trauma, the dental pulp mesenchymal stem cells must proliferate, and migrate to the area of injury for repairing. Therefore, blocking PrP expression could potentially promote more rapid cell proliferation and pulp healing, including the formation of secondary dentin. The cellular mechanism of PrP regulation of tooth organogenesis and repair will require further studies of the unique processes that promote stage-specific differentiation as the tooth develops.

Materials and Methods

Tissue samples

All human tissues were collected under the approval of the University of California San Francisco (UCSF) committee on human research. Developing human tooth organs were obtained from fetal cadaver tissues, obtained through the tissue-sharing program within UCSF.

Wild-type FVB mice were purchased from Charles River Laboratories (Wilmington, MA). PrP knockout mice (*Prnp*$^{0/0}$) have been previously described (Bueler *et al.,* 1992), and were on the FVB genetic background. Adult mice were euthanized by CO_2 asphyxiation, followed by decapitation, and newborn mice were euthanized by decapitation.

Immunohistochemical localization of PrP in the developing human and mouse incisors

Maxillas containing tooth organs from 21–24 week-old human fetal tissues, and heads from newborn *wt* and *Prnp*$^{0/0}$ mice, were collected and stored in 20% sucrose solution for 24 hr. The tissues were embedded and frozen in OCT compound (Tissue-Tek, USA), and cryosectioned at a thickness of 12 μm. The sections were fixed with 95% methanol and 5% acetic acid for 20 min at -20°C. Non-specific antibody binding was blocked with 3% bovine serum albumin for 30 min at room temperature, followed by washing in PBS with mild shaking for 5 min, 3 times. Slides were incubated with goat anti-PrP antibody (sc-7693, Santa Cruz Biotechnology INC, CA) for 48 hr at 4$^{°}$C, followed 3 washes in PBS. The slides were then incubated with secondary antibody (FITC conjugated anti-goat IgG) for 1 h in the dark at room temperature, washed, and counterstained with 0.5ug/mL Hoechst 33324 (Invitrogen, CA) for 5 min. Slides were mounted, observed, and photographed with Nikon Eclipse E800 fluorescent microscope.

The effect of PrP on undifferentiated dental mesenchymal cells in vitro

Pregnant mice were euthanized by standard carbon dioxide asphyxiation at the 18th day of gestation and the mandibular molar tooth buds were microdissected from the embryos under a dissecting microscope (Nikon SMZ 1500) in cold Hank's buffer. The tooth tissues were digested with 2mg/ml collagenase/dispase for 2 hr at 37$^{°}$C, followed by further digestion with STV (0.05% trypsin, 0.025% versene) for 5 min. Pulp dental mesenchymal cells (DMCs) were selectively grown in DMEM H-16 medium supplemented with 10% fetal bovine serum (Invitrogen, CA) and 1% penicillin-streptomycin at 37$^{°}$C, 5% CO_2.

To analyze the role of PrP on pulp cell proliferation, DMCs from *wt* and *Prnp*$^{0/0}$ mice were plated at 5,000 cells/well in a 96-well plate and grown in DMEM, 10% FBS, 1% PS at 37$^{°}$C, 5% CO_2 for 2 days. The cells were then synchronized in serum free DMEM for 24 hr and the media was then replaced with DMEM, 10% FBS and 1% PS, 10 μl BrdU and incubated for 24 hr. BrdU incorporation was compared using a BrdU chemiluminescence assay (Roche Applied Science, IN), according to the manufacturer's instructions.

To determine the effect of PrP on cell differentiation *in vitro*, DMCs from

E18 *Prnp*$^{0/0}$ *and wt* mice were grown in mineralization media including DMEM, 10% FBS, 1% PS, 10 mM β-glycerophosphate, 10 nM dexamethasone, and 50 μg/uL ascorbic acid for 2 wks. Von Kossa staining was used to identify mineral formation by first washing the cells with PBS, then fixing them in 2% glutaraldehyde for 15 min, washing, and then incubating the cells in 5% $AgNO_3$ solution for 30 min in the dark. The staining was revealed by ultraviolet exposure for 1 hr.

Characterization of dentin and enamel matrix formation in Prnp$^{0/0}$ *and wt teeth*

Mandibles of newborn mice were dissected out under a stereo-microscope, fixed in 10% neutral-buffered formalin overnight, rinsed with PBS, and dehydrated in a series of graded alcohols. The mandibles were then embedded in paraffin, and serially cross-sectioned at 7μm thickness. Some sections were stained with Masson's trichrome (Hebling *et al.,* 1999), with adjacent sections analyzed following von Kossa staining or immunolocalization of type I collagen, decorin or osteopontin.

For von Kossa staining, sections were dewaxed and incubated in 5% silver nitrate for 20 min. After washing with distilled water three times, the sections were incubated in 5% sodium thiosulfate for 2 min, followed by washing in distilled water and then dehydrated in a gradient series of alcohols.

Type I collagen was immunolocalized by first incubating the sections with 1 mg/ml hyaluronidase for 48 hr, rinsing with Walpole's buffer (sodium acetate 1.17% w/v, brought to pH 4.5 with glacial acetic acid) followed by PBS, and then incubating with rabbit type I collagen antibody (Chemicon International, CA) overnight at 4°C. The sections were then rinsed 3 times, incubated 1.5 hr with the peroxidase conjugated secondary anti-rabbit antibody (Dako, Denmark), and visualized with diaminobenzidine substrate (DAB, Sigma, MO).

Decorin, a small leucine-rich proteoglycan (SLRPs) noncollagenous protein, was immunodetected after pretreatment of the sections with chondroitinase ABC (Sigma, 0.25U/mL Tris/NaCl, pH 8) for 20 min at 37°C, to activate antigenic sites. After rinsing with PBS, the sections were incubated with rabbit anti-decorin antibody (LF113, generous gifts from Larry Fisher, NIDCR) and detected by DAB as described above. Osteopontin was detected after incubation with anti-OPN antibody (LF123, generous gift from Larry Fisher, NIDCR).

Analyses of gene expression in odontoblasts isolated by microdissection

Laser capture microdissection (LCM) was done using a PALM Microlaser system® (Leica). Newborn mouse mandibles (*wt* and *ko*) were fresh frozen, embedded in OCT, and cryosectioned at -18 °C with a thickness of 12 μm. The sections were mounted on polyethylene naphthalate (PEN) foil glass slides (Leica) with 8 sections per slide. After H&E staining, the slides were air-dried, and pre-odontoblasts (POB) and secretory odontoblasts (SOB) were separately dissected and catapulted to microtube caps designed for the PALM system. The caps with the collected cells were placed on microtubes containing 50 μl lysis buffer stock solution (49.3 μL RLT buffer + 0.5 μL β-ME +0.2 μL Linear acrylamide), and briefly vortexed upside down. RNA purification was done with RNeasy Plus Micro Kit (Qiagen, CA), and reverse transcription was done with Super Script III (Invitrogen, CA), following the manufacturer's instructions. Quantitative PCR (qPCR) was done using an Applied Biosystems 7500 (Applied Biosystems Inc., CA) with specific primers to amplify PCNA, type I collagen, and dentin sialophosphoprotein (DSPP) mRNA.

Microhardness of molar enamel and dentin

Mandibles from 2-month old male mice were embedded in epoxy resin and sagittally ground to the mid-section of the first molars. A flat and highly polished surface was generated using graded series of polishing grit in order to establish orthogonality with the indenter tip (Ho *et al.,* 2004). Microindentation was performed on enamel, dentin (coronally and apically), and predentin (around the pulp chamber and root canal space) under dry conditions using a Knoop diamond indenter (Buehler Ltd., Lake

Bluff, IL) and a normal load of 10gram force. Each indent was identified using a light microscope and the long diagonal measured using Image-Pro data-acquisition software (Image-Pro Plus Microscope, version 4.0; Media Cybernetics, Silver Spring, MD). Microhardness was determined by: HK = $0.014229P/D^2$ where HK is the Knoop microhardness in gigapascal (GPa), P is the normal load in Newtons (N) and D is the length of long diagonal in millimetres (mm).

Stereomicroscopic and microCT analyses of enamel mineralization

Mandibles from two-month-old adult male mice were separated into 2 hemimandibles. The left hemimandible from each mouse was embedded in epoxy resin and ground sagittally to the central plane of the incisor using 600 grit silicon carbide paper, photographed under a stereomicroscope, and compared. Enamel formation was characterized by the length of the white opaque enamel zone at the lingual surface of incisors, ending when the more mineralized enamel took on a more translucent color.

Right dry hemimandibles were scanned with a microCT (micro x-ray computed tomography unit; SkyScan 1076®, Belgium) to characterize the mineral density of the dental tissues in *wt* and *Prnp*$^{0/0}$ mice. Scans were done at 100 kVp, 100 µA with a resolution of 8.87µm. 2D sections were stored in a bmp format with indexed gray levels ranging from 0 (black) to 255 (white). DataViewer software (ver 1.4.1 SkyScan) was used to locate a midsagittal plane, which was then used for densitometry (g/cm^2) analysis. A cross-sectional plane was taken through the incisor perpendicular to the mesial root of the first molar, and the density of the enamel in the *wt* and *Prnp*$^{0/0}$ mice was compared.

References

AGUZZI A, BAUMANN F, BREMER J (2008). The prion's elusive reason for being. *Annu Rev Neurosci* 31: 439-477.

BEI M, MAAS R (1998). FGFs and BMP4 induce both Msx1-independent and Msx1-dependent signaling pathways in early tooth development. *Development* 125: 4325-4333.

BERALDO FH, ARANTES CP, SANTOS TG, QUEIROZ NG, YOUNG K, RYLETT RJ *et al.,* (2010). Role of alpha7 nicotinic acetylcholine receptor in calcium signaling induced by prion protein interaction with stress-inducible protein 1. *J Biol Chem* 285: 36542-36550.

BREMER J, BAUMANN F, TIBERI C, WESSIG C, FISCHER H, SCHWARZ P *et al.,* (2010). Axonal prion protein is required for peripheral myelin maintenance. *Nat Neurosci* 13: 310-318.

BUELER H, FISCHER M, LANG Y, BLUETHMANN H, LIPP HP, DEARMOND SJ *et al.,* (1992). Normal development and behaviour of mice lacking the neuronal cell-surface PrP protein. *Nature* 356: 577-582.

BUELER H, AGUZZI A, SAILER A, GREINER RA, AUTENRIED P, AGUET M *et al.,* (1993). Mice devoid of PrP are resistant to scrapie. *Cell* 73: 1339-1347.

CAUGHEY B, RACE RE, CHESEBRO B (1988). Detection of prion protein mRNA in normal and scrapie-infected tissues and cell lines. *J Gen Virol* 69 (Pt 3): 711-716.

CHIESA R, HARRIS DA (2009). Fishing for prion protein function. *PLoS Biol* 7: e75.

COLLINGE J, WHITTINGTON MA, SIDLE KC, SMITH CJ, PALMER MS, CLARKE AR *et al., (*1994). Prion protein is necessary for normal synaptic function. *Nature* 370: 295-297.

FUHRMANN M, BITTNER T, MITTEREGGER G, HAIDER N, MOOSMANG S, KRETZSCHMAR H *et al.* (2006). Loss of the cellular prion protein affects the Ca2+ homeostasis in hippocampal CA1 neurons. *J Neurochem* 98: 1876-1885.

HARADA H, KETTUNEN P, JUNG HS, MUSTONEN T, WANG YA, THESLEFF I (1999). Localization of putative stem cells in dental epithelium and their association with Notch and FGF signaling. *J Cell Biol* 147: 105-120.

HEBLING J, GIRO EM, COSTA CA (1999). Human pulp response after an adhesive system application in deep cavities. *J Dent* 27: 557-564.

HO SP, BALOOCH M, MARSHALL SJ, MARSHALL GW (2004). Local properties of a functionally graded interphase between cementum and dentin. *J Biomed Mater Res A* 70: 480-489.

ICHIKAWA J, GEMBA H (2009). Cell density-dependent changes in intracellular Ca2+ mobilization via the P2Y2 receptor in rat bone marrow stromal cells. *J Cell Physiol* 219: 372-381.

KAGENISHI T, YOKAWA K, KUSE M, ISOBE M, BOUTEAU F, KAWANO T (2009). Prevention of copper-induced calcium influx and cell death by prion-derived peptide in suspension-cultured tobacco cells. *Z Naturforsch C* 64: 411-417.

KHAN QE, PRESS CM, SEHIC A, LANDIN MA, RISNES S, OSMUNDSEN H (2010). Expression of prion gene and presence of prion protein during development of mouse molar tooth germ. *Eur J Oral Sci* 118: 559-565.

LAZARINI F, DESLYS JP, DORMONT D (1991). Regulation of the glial fibrillary acidic protein, beta actin and prion protein mRNAs during brain development in mouse. *Brain Res Mol Brain Res* 10: 343-346.

LE PICHON CE, VALLEY MT, POLYMENIDOU M, CHESLER AT, SAGDULLAEV BT, AGUZZI A *et al.,* (2009). Olfactory behavior and physiology are disrupted in prion protein knockout mice. *Nat Neurosci* 12: 60-69.

LEE YJ, BASKAKOV IV (2010). Treatment with normal prion protein delays differen-tiation and helps to maintain high proliferation activity in human embryonic stem cells. *J Neurochem* 114: 362-373.

LI R, LIU D, ZANUSSO G, LIU T, FAYEN JD, HUANG JH *et al.,* (2001). The expres-sion and potential function of cellular prion protein in human lymphocytes. *Cell Immunol* 207: 49-58.

LLEDO PM, TREMBLAY P, DEARMOND SJ, PRUSINER SB, NICOLL RA (1996). Mice deficient for prion protein exhibit normal neuronal excitability and synaptic transmission in the hippocampus. *Proc Natl Acad Sci USA* 93: 2403-2407.

MANDLER M, NEUBUSER A (2001). FGF signaling is necessary for the specification of the odontogenic mesenchyme. *Dev Biol* 240: 548-559.

MANSON J, WEST JD, THOMSON V, MCBRIDE P, KAUFMAN MH, HOPE J (1992). The prion protein gene: a role in mouse embryogenesis? *Development* 115: 117-122.

MANSON JC, CLARKE AR, HOOPER ML, AITCHISON L, MCCONNELL I, HOPE J (1994a). 129/Ola mice carrying a null mutation in PrP that abolishes mRNA production are developmentally normal. *Mol Neurobiol* 8: 121-127.

MANSON JC, CLARKE AR, MCBRIDE PA, MCCONNELL I, HOPE J (1994b). PrP gene dosage determines the timing but not the final intensity or distribution of lesions in scrapie pathology. *Neurodegeneration* 3: 331-340.

MCKINLEY MP, HAY B, LINGAPPA VR, LIEBERBURG I, PRUSINER SB (1987). Developmental expression of prion protein gene in brain. *Dev Biol* 121: 105-110.

MENICANIN D, BARTOLD PM, ZANNETTINO AC, GRONTHOS S. (2010). Identifi-cation of a common gene expression signature associated with immature clonal mesenchymal cell populations derived from bone marrow and dental tissues. *Stem Cells Dev* 19: 1501-1510.

NEUBUSER A, PETERS H, BALLING R, MARTIN GR (1997). Antagonistic interac-tions between FGF and BMP signaling pathways in positioning the sites of tooth formation. *Cell* 90: 247-255.

OKADA H, SAKURAI M, YOKOYAMA T, MOHRI S (2010). Disease-Associated Prion Protein in the Dental Tissue of Mice Infected with Scrapie. *J Comp Pathol.*

POWELL AD, TOESCU EC, COLLINGE J, JEFFERYS JG (2008). Alterations in Ca2+-buffering in prion-null mice: association with reduced afterhyperpolarizations in CA1 hippocampal neurons. *J Neurosci* 28: 3877-3886.

PREMZL M, GAMULIN V (2007). Comparative genomic analysis of prion genes. *BMC Genomics* 8: 1.

PRUSINER SB, GROTH D, SERBAN A, KOEHLER R, FOSTER D, TORCHIA M *et al.,* (1993). Ablation of the prion protein (PrP) gene in mice prevents scrapie and facilitates production of anti-PrP antibodies. *Proc Natl Acad Sci USA* 90: 10608-10612.

SCHNEIDER K, KORKMAZ Y, ADDICKS K, LANG H, RAAB WH (2007). Prion pro-tein (PrP) in human teeth: an unprecedented pointer to PrP's function. *J Endod* 33: 110-113.

SHARPE PT (2001). Neural crest and tooth morphogenesis. *Adv Dent Res* 15: 4-7.

THESLEFF I, NIEMINEN P (1996). Tooth morphogenesis and cell differentiation. *Curr Opin Cell Biol* 8: 844-850.

TREMBLAY P, BOUZAMONDO-BERNSTEIN E, HEINRICH C, PRUSINER SB, DEARMOND SJ (2007). Developmental expression of PrP in the post-implantation embryo. *Brain Res* 1139: 60-67.

VAAHTOKARI A, ABERG T, THESLEFF I (1996). Apoptosis in the developing tooth: association with an embryonic signaling center and suppression by EGF and FGF-4. *Development* 122: 121-129.

WADDINGTON RJ, HALL RC, EMBERY G, LLOYD DM (2003). Changing profiles of proteoglycans in the transition of predentine to dentine. *Matrix Biol* 22: 153-161.

Further Related Reading, published previously in the *Int. J. Dev. Biol.*

Contribution of mesoderm to the developing dental papilla
Michaela Rothová, Jifan Feng, Paul T. Sharpe, Renata Peterková and Abigail S. Tucker
Int. J. Dev. Biol. (2011) 55: 59-64

Induction of neural crest cells from mouse embryonic stem cells in a serum-free monolayer culture
Yuko Aihara, Yohei Hayashi, Mitsuhi Hirata, Nobutaka Ariki, Shinsuke Shibata, Narihito Nagoshi, Mio Nakanishi, Kiyoshi Ohnuma, Masaki Warashina, Tatsuo Michiue, Hideho Uchiyama, Hideyuki Okano, Makoto Asashima and Miho Kusuda Furue
Int. J. Dev. Biol. (2010) 54: 1287-1294

BMP signalling in craniofacial development
Xuguang Nie, keijo Luukko and Paivi Kettunen
Int. J. Dev. Biol. (2006) 50: 511-521

Study of novel genes involved in odontoblast and ameloblast differentiation
FJ Unda, N Iehara, S De-Vega, M De-La-Fuente, A Vilaxa, Y Yamada
Int. J. Dev. Biol. (2001) 45: 9910-9910

Differential expression of laminin-5 subunits during incisor and molar development in the mouse
K Yoshiba, N Yoshiba, D Aberdam, G Meneguzzi, F Perrin-Schmitt, C Stoetzel, J V Ruch and H Lesot
Int. J. Dev. Biol. (2000) 44: 337-340

5 yr ISI Impact Factor (2010) = 2.961